ELSEVIER

Catalysis Today 78 (2003) 487–498

CATALYSIS TODAY

www.elsevier.com/locate/cattod

Epoxidation of cyclohexene on Nb-containing meso- and macroporous materials

Izabela Nowak, Beata Kilos, Maria Ziolek*, Anna Lewandowska

Faculty of Chemistry, A. Mickiewicz University, Grunwaldzka 6, PL-60-780 Poznan, Poland

Abstract

Various niobium-containing meso- and macroporous materials were prepared and characterised by means of XRD and H_2-TPR techniques, scanning electron microscopy (SEM), and sorption measurements. They were tested in the liquid phase oxidation of cyclohexene to epoxide with hydrogen peroxide. The effect of various parameters such as a nature of solvent, material structure, atmosphere on the activity and selectivity of the reaction was studied. NbMCM-41 and NbSM-2 materials are highly active in the epoxidation.

Keywords: NbMCM-41; NbSM-1; NbSM-2; Epoxidation; Cyclohexene

1. Introduction

A novel family of mesoporous molecular sieves designated as M41S was discovered in 1992 [1]. These materials, initially synthesised in aluminosilicate and purely siliceous forms, are characterised by a very large surface area (1000–1400 $m^2\,g^{-1}$) and a very narrow pore size distribution (PSD). There is a well-defined porous phase in this family of materials—namely MCM-41 molecular sieve with a hexagonal arrangement of mono-dimensional pores [2]. Owing to their exceptional adsorption capacities and molecular sieving properties, they are very attractive materials for the design of new heterogeneous catalysis. Acidic and redox functions important in catalysis can be generated by the incorporation of heteroelements as extra-framework nanoscale oxide clusters or in their appropriate valence state as tetrahedral framework species. Recently, Nb-modified molecular sieves of M41S family have been recognised as very attractive catalysts in the oxidation of organic compounds with hydrogen peroxide [3,4].

In this work we wish to report the results of cyclohexene epoxidation on Nb-containing MCM-41 prepared according to various procedures, NbSM-1, and NbSM-2. Among the advantages proposed for these types of solids are the presence of a regular porous system and the large pore size. Thus the comparison has been made regarding the differences in the pore size and uniformity of the pore size distribution (PSD).

2. Experimental

2.1. Sample preparation

A few different methods have been applied for the synthesis of meso/macroporous niobosilicates sam-

---

* Corresponding author. Tel.: +48-61-829-1243; fax: +48-61-865-8008.
E-mail address: ziolek@amu.edu.pl (M. Ziolek).

0920-5861/02/$ – see front matter © 2002 Elsevier Science B.V. All rights reserved.
PII: S0920-5861(02)00332-2

ples. They are as follows: (i) a hydrothermal synthesis in the PP bottles (as in [5]) or in the autoclave (adopted from [6]), (ii) a novel rapid synthesis at room temperature (RT) according to [7], and (iii) a synthesis under the static conditions described in [8]. In all synthesised materials the molar Si/Nb ratio was assumed to be 32.

The procedures of each type of synthesis are given below:

1. NbMCM-41 materials were synthesised according to the procedure described earlier [5]. A quantity of 8.08 g of sodium silicate (27% SiO_2 in 14% NaOH; Aldrich) was added to 50 g of distilled water under stirring. A 83.75 g of a template/water mixture (25 wt.%, hexadecyltrimethylammonium chloride; Aldrich) was added after 10 min. Then 6.03 g of niobium oxalate solution in 0.1 M oxalic acid (0.6036 g of niobium(V) oxalate; CBMM, Brazil) was slowly added for achieving Si/Nb = 32. The pH of the formed gel was adjusted to 11 and stirred for about 0.5 h before 20 g of distilled water was added. The gel was loaded into a stoppered PP bottle and heated without stirring at 373 K for 24 h. The mixture was then cooled to RT and the pH was again adjusted to 11. This reaction mixture was heated again to 373 K for 24 h. Afterwards, two different procedures have been applied: (i) in the first, the formed solid was filtered, extensively washed with a large amount of distilled water, dried at RT for 30 min on filter and then at 333 K in the oven, (ii) in the second, the precipitated product was recovered by filtration, washed with a small volume of distilled water and dried at 333 K in the oven. The products were finally calcined at 773 K for 2 h in helium flow and then for 15 h under static conditions in air. These samples, depending on the procedure of synthesis and the uniformity of material formed (shown below), will be denoted as NbMCM-41(UPS) in the first case and NbMCM-41(NUPS) in the second one.
2. Novel synthesis at RT (the prepared material denoted NbMCM-41(RT)) was performed according to the procedure described by Schumacher et al. [7]. *N*-hexadecyltrimethylammonium bromide (2.4 g; Acros) was dissolved in distilled water (50 g) and ethanol (98 vol.%, 50 cm^3; Polmos, Poland), and aqueous ammonia (32 wt.%, 15.3 cm^3; POCh, Poland) was added to the surfactant solution. The solution was stirred for 10 min and tetraethoxysilane—TEOS (98 wt.%, 3.4 g; Aldrich) and a source of niobium (niobium(V) oxalate = 0.27 g; CBMM, Brazil) were added. After stirring for 2 h at RT the resulting solid was recovered by filtration, washed with distilled water and dried in air at ambient temperature. The template was removed by calcination at 823 K for 8 h.
3. Hydrothermal synthesis in autoclave led to the formation of meso/macroporous niobosilicate-1 denoted as NbSM-1. It was synthesised according to the modified procedure described by Sayari [6]. Tetramethylammonium hydroxide (25 wt.%, 3.85 g; Aldrich) was diluted with water (37.1 g) before adding *n*-hexadecyltrimethylammonium bromide (3.04 g; Acros) under vigorous stirring. After 15 min of stirring, Cab–O–Sil silica (2 g; BDH) and a source of niobium (niobium(V) oxalate = 0.55 g; CBMM, Brazil) were added. The gel, after stirring for an additional 30 min, was transferred into a Teflon lined autoclave and heated statically (under autogeneous pressure) for 40 h at 403 K. The product was filtered, washed with water, and dried at RT. Finally, the template was removed by heating at 773 K in helium for 2 h and then in air for 12 h.
4. NbSM-2 (macroporous niobosilicate) was obtained by modifying the procedure described in the paper of Maschmeyer and co-workers [9]. Ageing, drying, and calcining a homogeneous basic synthesis mixture composed of niobium source, silicon source—TEOS, and template: TEA (triethanolamine) were applied.

Niobium was incorporated to the catalysts not only during the synthesis but also via the impregnation of siliceous MCM-41 with niobium(V) oxalate.

Ti-, V- and NbVMCM-41 molecular sieves were prepared in similar way as this described in method I, with the exception that sources of vanadium or titanium were used instead of niobium in the first two cases or vanadium together with niobium in the latter sample. The molar Si/T ratio was always kept as 32.

All catalysts used in this work and their physicochemical data are given in Table 1.

Table 1
The physico-chemical data of the catalysts used in this work

Catalyst	*d* spacing (nm)	Surface area ($m^2\,g^{-1}$)	Pore volume ($cm^3\,g^{-1}$)	Average pore diameter (nm)
NbMCM-41(NUPS)	3.94	1035	1.19	3.42
NbMCM-41(UPS)	3.68	1024	1.04	3.14
Nb/MCM-41	–	967	1.45	4.95
NbMCM-41(RT)	3.24	1540	0.99	2.58
NbMS-1	[a]	285	1.75	24.69[b]
NbMS-2	[a]	206	0.66	12.76[b]
VMCM-41	3.62	992	1.09	3.48
TiMCM-41	3.74	852	1.19	4.36
NbVMCM-41	4.51	1059	1.69	5.13

[a] Not possible to determine.
[b] Macropores.

2.2. Sample characterisation

2.2.1. Powder X-ray diffraction (XRD)

The XRD patterns of the materials after synthesis and calcination were acquired on a TUR 42 powder diffractometer using nickel-filtered Cu Kα radiation (10 kV, 40 mA) and a step size 0.02°.

2.2.2. Nitrogen sorption

The nitrogen adsorption/desorption isotherms were measured at 77 K on a Micromeritics ASAP 2010 volumetric adsorption analyser. Before measurements, the samples were outgassed at 573 K for 3 h in the degas port of the adsorption instrument. The volume of adsorbed N_2 was normalised to the standard temperature and pressure. The BET surface area was calculated with the cross-sectional area of nitrogen molecule taken as $1.62\,nm^2$ by applying the BET equation for relative pressure between 0.05 and 0.22. The PSD was calculated using the desorption branch of the N_2 adsorption/desorption isotherm and the Barret–Joyner–Halenda (BJH) formula. The cumulative pore volume (V_{BJH}) of the mesopores was obtained from the PSD curve.

2.2.3. Temperature programmed reduction (TPR) studies

H_2-TPR was performed in a fixed-bed quartz reactor with a Micromeritics 2705 chemisorption analyser. Prior to the reduction experiment, the samples (∼40 mg) were activated in a helium flow at 723 K at a rate of $10\,K\,min^{-1}$. After the sample was cooled to RT in He, the reduction of samples was carried out from 303 to 1373 K in a flow of 10 vol.% H_2 in Ar at $10\,K\,min^{-1}$. The consumption of H_2 was monitored continuously with a thermal conductivity detector.

2.2.4. Scanning electron microscopy

Scanning electron microscopy (SEM) was performed using a Philips SEM 515.

2.3. Epoxidation of cyclohexene

All prepared materials were tested in the oxidation of cyclohexene with hydrogen peroxide. The reaction was performed at 318 K in the liquid phase using various solvents (methanol, *t*-butanol, acetone and acetonitrile) in the case of NbMCM-41(NUPS), and acetonitrile only in the study of other samples. The catalytic reaction between cyclohexene and hydrogen peroxide was carried out in a glass flask equipped with a magnetic stirrer, a thermocouple, a reflux condenser, and a membrane for sampling. A 0.04 g of a calcined catalyst was placed in the flask where the solvent was added. The oxidation was conducted simply by efficient stirring of a mixture of solvent and a catalyst at 318 K. After stirring for 15 min, cyclohexene (2 mmol) was added, followed by the dropwise addition of 34 vol.% hydrogen peroxide (2 mmol).

The reaction mixtures were analysed each 30 min with Chrom-5 chromatograph equipped with a packed column of SP-2340 operated with the heating program: 333 K for 4 min, ramp $12\,K\,min^{-1}$ to 411 K (kept for 6 min), ramp $15\,K\,min^{-1}$ to 493 K (kept for 12 min). A flame ionisation detector (FID) was applied. The first analysis was done after 30 min from the beginning of the reaction. Additionally, the GC-MS (AMD 402) analyses were performed in order to identify the reaction products.

Moreover, the reaction was conducted in the homogeneous phase, i.e. in the solution of niobium(V) oxalate in acetonitrile or methanol (the concentration of Nb in the solution was equivalent to that one which could be obtained if the whole niobium from a 0.04 g NbMCM-41 (Si/Nb = 32) is leached to the reaction solution).

In order to find whether the radical mechanism is involved in the studied reaction, the epoxidation was performed after saturation of the catalyst, mixed with solvent, with nitrogen oxide.

3. Results

3.1. Structure and texture characterisation

The calcined NbMCM-41 materials (NUPS and UPS) gave well-defined hexagonal XRD patterns with a main peak (indexed assuming a hexagonal unit cell as [1 0 0]) at $2\theta \approx 2^\circ$ and up to three signals in the region $2\theta = 3$–8°. These reflections are due to the ordered hexagonal array of parallel silica tubes. The XRD patterns of these materials are shown in Fig. 1. NbMCM-41(RT) shows broader [1 0 0] interference than samples prepared by conventional method. In the case of NbSM-1 and NbSM-2 the XRD patterns do not exhibit the reflections characteristic of MCM-41 mesoporous molecular sieves.

Scanning electron images of some samples are shown in Fig. 2. Non-agglomerated uniform spheres were achieved by the preparation of NbMCM-41 material at RT, while irregularly shaped particles where obtained by the hydrothermal synthesis—NbMCM-41(UPS). The boundaries among mesoporous particles appear in the sample NbSM-1. NbSM-2 sample shows irregular morphology.

The nitrogen sorption isotherms of NbMCM-41 samples (Fig. 3A) are of type IV in the IUPAC classification and show a distinct feature: a sharp capillary condensation step at a relative pressure of ~0.35 for samples NbMCM-41(UPS) and NbMCM-41(NUPS)—Fig. 3A. The hysteresis loop is observed in the p/p_0 range close to the saturation pressure for both samples. However, the biggest one is exhibited for the latter one. This sample shows double mesoporous system with pore diameters of 3 and 4 nm (Fig. 4A). No hysteresis loop was detected for NbMCM-41(RT), which proves the high quality mesoporous framework. However, the pores are slightly smaller (as seen from PSD—Fig. 4A). It is worthy to note that for all MCM-41 samples one can observe very high adsorption in mesoporous region (plateau at ~500 $\mathrm{cm^3\,g^{-1}}$).

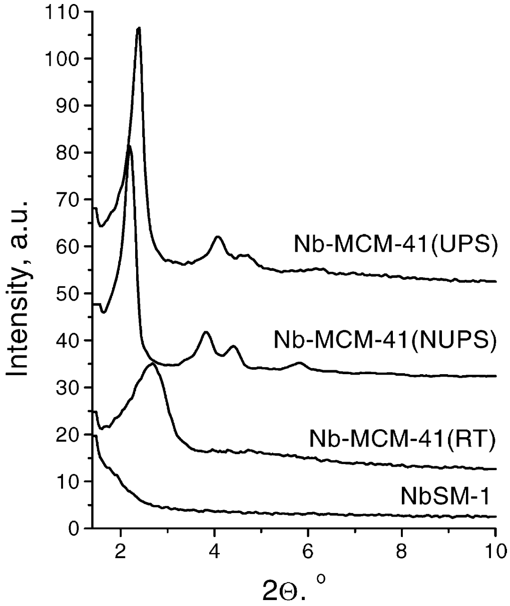

Fig. 1. XRD patterns of samples used in this work.

NbSM-1 material shows unusual shape of the isotherm (Fig. 3B)—there is some shape of type IV retained, however: (i) the condensation step is not sharp, (ii) the plateau is observed at 200 $\mathrm{cm^3\,g^{-1}}$ which is in agreement with the small surface area and (iii) at $p/p_0 = 0.9$ the very high increase of the adsorbed volume is noticed. However, one can see for that sample biporous—meso-macro-system—with pore diameters of 2.7 and 33.0 nm. The second macroporous material—NbSM-2 shows as well visible double porous system, but in this case they are macropores with diameter of 6.0 and 15.2 nm. The average pore diameters presented in Table 1 do not characterise well the porosity of the materials because they consist of two various pore sizes in some samples, whereas for the others they base on one pore system.

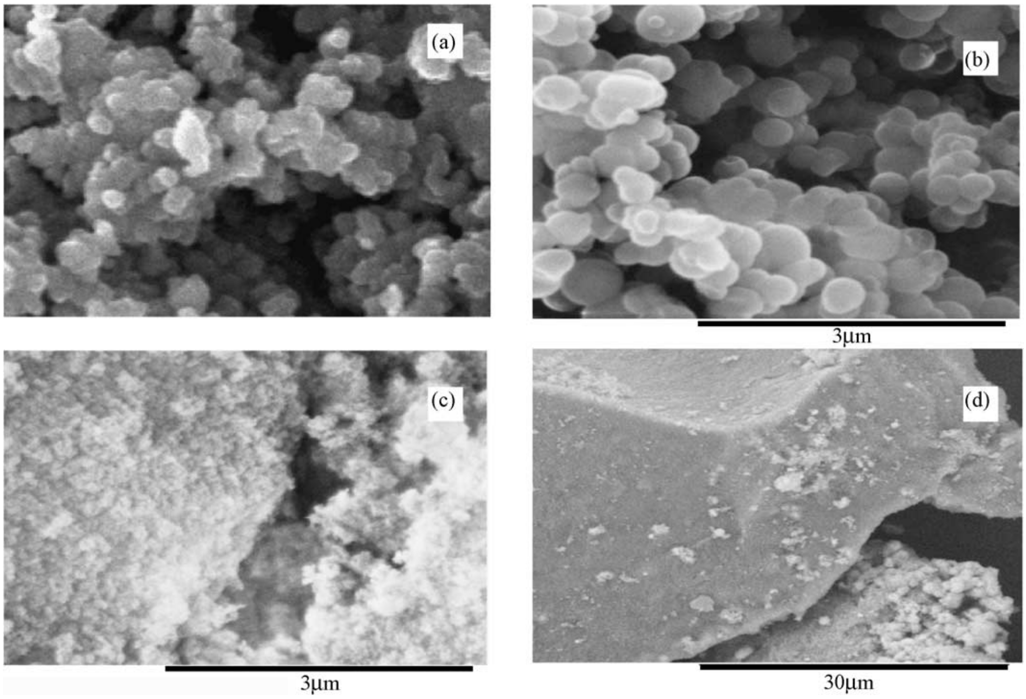

Fig. 2. SEM micrographs of the following samples: (a) NbMCM-41(UPS); (b) NbMCM-41(RT); (c) NbSM-1 and (d) NbSM-2.

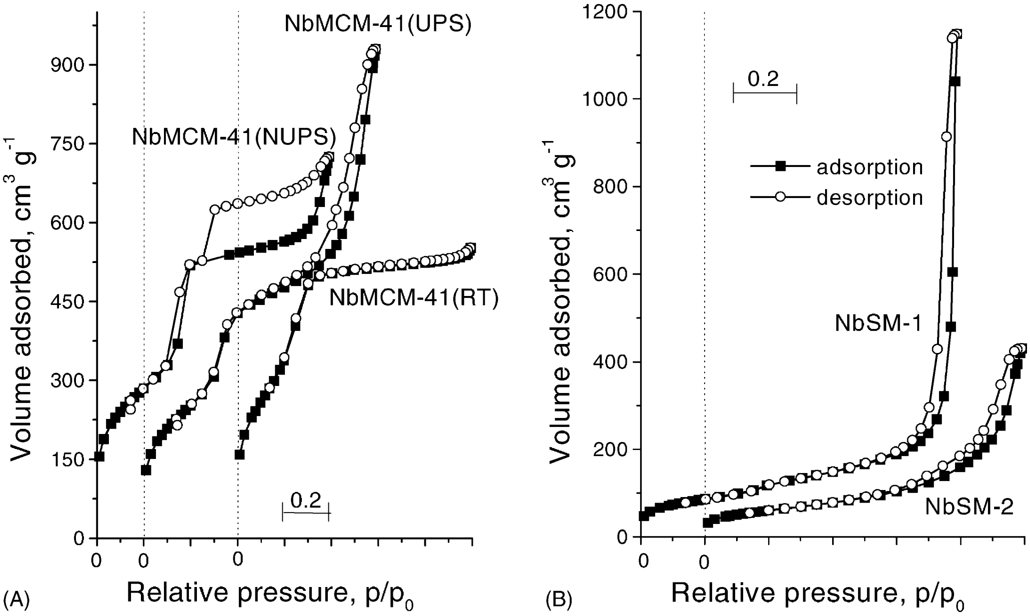

Fig. 3. N_2 adsorption/desorption isotherms for NbMCM-41 samples (A) and NbSM-1 and NbSM-2 (B).

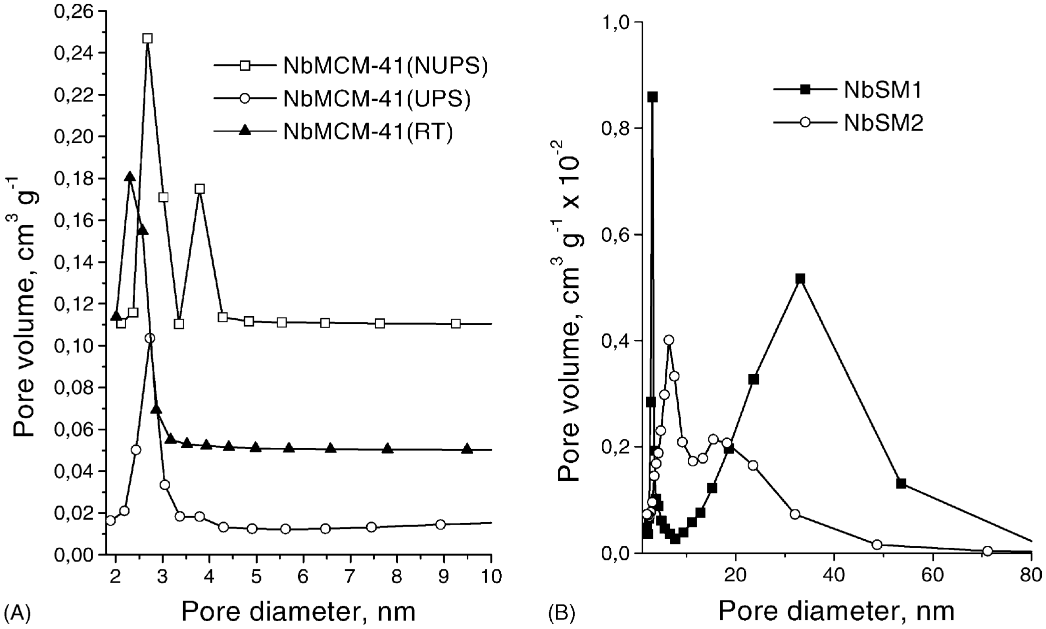

Fig. 4. PSD for NbMCM-41 samples (A) and NbSM-1 and NbSM-2 (B).

All MCM-41 type materials exhibit very high surface areas (above 1000 $m^2\ g^{-1}$, excepting the impregnated sample)—Table 1. Among them the highest value (for samples prepared by the hydrothermal type of synthesis) is noted in the case of bi-heteroelements material, i.e. NbVMCM-41. The surface area of other samples strongly depends on the preparation method.

The H_2-TPR profiles of mesoporous Nb-MCM-41(RT), meso-macroporous NbSM-1, and macroporous NbSM-2 are exhibited in Fig. 5. It is known [12] that the low temperature (LT) peaks (below 1000 K) are due to the reduction of extra framework niobium species, whereas, those at high temperatures (HTs) above 1000 K characterise the reduction of niobium localised in the framework. Two well-resolved H_2-TPR peaks above 1000 K registered for NbSM-2 are like those observed for niobosiliceous MCM-41 material and were assigned to NbO^- and Nb^+ species connected with the silica tetrahedra [12]. This observation allows the suggestion about the incorporation of niobium into the siliceous framework in NbSM-2. NbSM-1 material did not give a clearly defined H_2-TPR profile. NbMCM-41(RT) mesoporous molecular sieve exhibits both kinds of niobium species: ex-

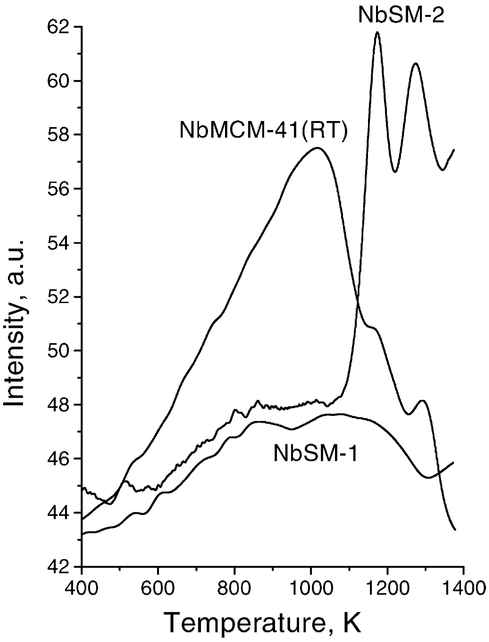

Fig. 5. H_2-TPR profiles.

tra framework reduced at LT and framework reduced at HT with the domination of the first one.

3.2. Epoxidation of cyclohexene

Recently, niobium-containing mesoporous molecular sieves of MCM-41 type have been recognised as very active catalysts in the oxidation of cyclohexene [4,10]. The reaction takes usually more than 30 h. This reaction carried out on NbMCM-41 mesoporous sieves reported in the earlier paper [4] has shown the selectivity towards glycol ether or glycol depending on the nature of solvent, the latter being formed in alcohols and the first in acetone. The authors conducted the reaction at 333 K. In our study we wish to obtain mainly epoxide. Therefore, we applied the lower reaction temperature (318 K) and various solvents: methanol, *t*-butanol, acetone and acetonitrile. The obtained results are summarised in Table 2.

The best solvent for the epoxidation of cyclohexene was acetonitrile as shown from the results obtained on NbMCM-41(NUPS) material—the highest selectivity (99%) towards epoxide was reached. Therefore, other samples were studied using mainly one solvent—acetonitrile. The application of methanol gives rise to the higher cyclohexene conversion (77%) on NbMCM-41(NUPS), however, the main product is glycol, not epoxide. The use of acetone as a solvent changes the selectivity of the reaction, which turns to the production of epoxide. The lowest conversion was observed in *t*-butanol on NbMCM-41. The latter is due to the diffusion effect caused by bulky molecules of solvent. It is worthy to notice that in the literature the highest selectivity to epoxide on Nb-catalysts was found on sodium tetraperoxoniobate, $Na_3[Nb(O_2)_4]\cdot 13H_2O$ (73% selectivity to epoxide) but the conversion was very low (7%) [11]. To conclude, alcohols applied as solvents cause the side reactions, i.e. the alkoxylation of cyclohexene. There are a few reaction pathways proposed in the literature for the oxidation of cyclohexene [3,5]. They are given in Scheme 1.

The products estimated in the reactions carried out on NbMCM-41(NUPS) indicate the domination of the reaction pathway no. 2.

The incorporation of vanadium as the second heteroelement besides niobium in MCM-41 sample increases the activity of the material and moves the selectivity from epoxide (dominated on NbMCM-41(NUPS)) to glycol (on NbVMCM-41) (Table 2).

The new material—NbSM-2, exhibits also a very high activity and selectivity to epoxide in the reaction studied. Fig. 6 compares the cyclohexene conversion on various niobium-containing catalysts. The highest conversion after 12 h is reached on NbSM-2, whereas the lowest induction period is characteristic of NbMCM-41(NUPS). Surprisingly, NbMCM-41(RT) with the highest surface area and a very good morphology presents a very low activity.

Table 2
Activity of meso/macroporous molecular sieves in oxidation of cyclohexene by hydrogen peroxide

Catalyst	Solvent	Maximum conversion (%)	Product distribution (%)		
			Epoxide	Glycol	Others[a]
NbMCM-41(NUPS)	Methanol	77	0	97	3
NbMCM-41(NUPS)	*t*-Butanol	19	0	82	18
NbMCM-41(NUPS)	Acetone	71	62	10	28
NbMCM-41(NUPS)	Acetonitrile	58	99	0	1
Nb/MCM-41	Acetonitrile	59	21	67	12
VMCM-41	Acetonitrile	0.2	0	45	55
TiMCM-41	Acetonitrile	0.5	–	–	–
NbVMCM-41	Acetonitrile	58	0.5	70	29.5
NbVMCM-41	Methanol	92	Traces	85	15
NbMCM-41(RT)	Acetonitrile	6	89	5.5	5.5
NbSM-1	Acetonitrile	78	96	0.7	2.3
NbSM-2	Acetonitrile	87	99.8	0.1	0.1

[a] Other products are 4-methyl-3-3-penten-2-one, 2-cyclohexen-1-ol, 2-cyclohexen-1-one, 2-hydroxycyclohexanone, *trans*-1,2-cyclohexanodiole, 7-oksobicyclo[4.1.0]heptane.

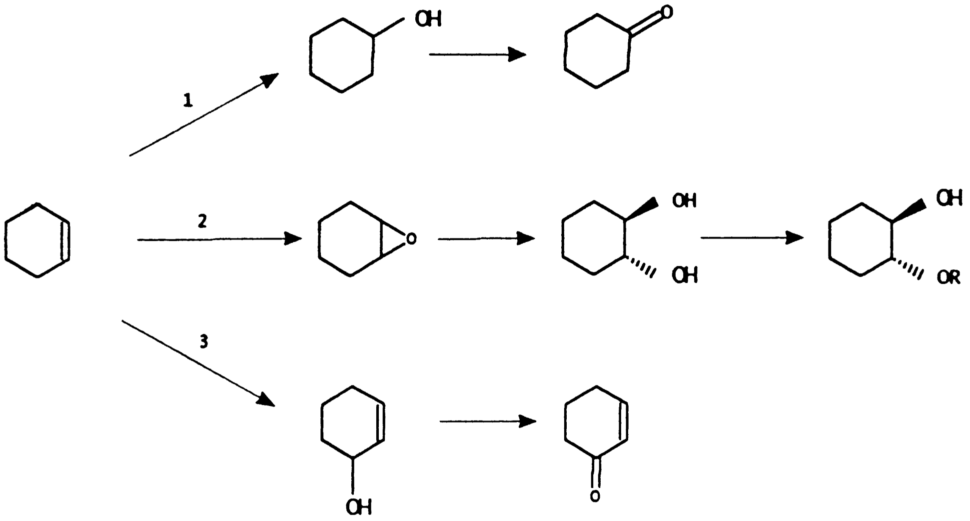

Scheme 1.

NbSM-1 sample containing both meso- and macropores exhibits a comparable activity to that one observed for NbMCM-41(RT) in the initial reaction time, but higher than the activity of all NbMCM-41 samples after 12 h of the reaction.

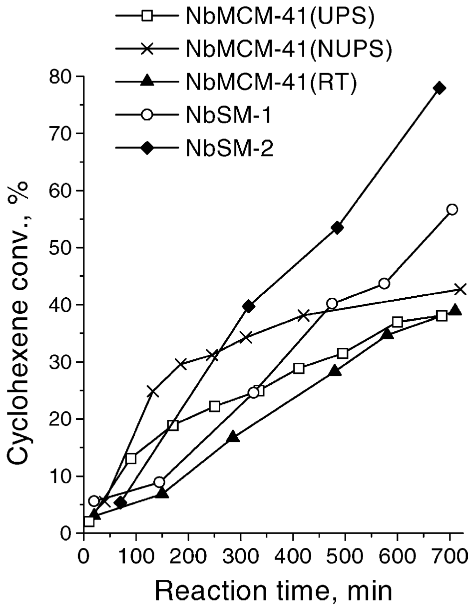

Fig. 6. Changes of cyclohexene conversion with time of the oxidation carried out in acetonitrile.

In the oxidation of large molecules it is important to use the catalysts with large and free pores which eliminate or reduce the diffusion effect. The pore diameters in NbMCM-41(UPS and NUPS) sieves are very high (see Table 1), and therefore, the diffusion does not seem to limit the reaction rate if the solvent molecules are not too bulky. However, samples containing only mesopores show less induction period than samples containing macropores. Maybe in macroporous materials the active species are less effective and require the activation in the initial stage of the process.

In the impregnated samples the pore diameter is lower due to the existence of extra framework niobium species, and the diffusion effect has to be considered. This effect can be responsible for the long induction period in the reaction conducted on the impregnated samples (Nb/MCM-41-32 and Nb/AlMCM-41-32)—Fig. 7. Due to the low activity at the beginning of the reaction, epoxide, which is most probably formed in the first step, is easily transformed to glycol.

The activity of Nb-containing materials was compared with that found on TiMCM-41 and VMCM-41. Both titanium and vanadium catalysts were less active than NbMCM-41 sieves. Moreover, vanadium was easily leached from the catalyst to the solution and therefore, the regeneration does not restore the former activity of the catalyst.

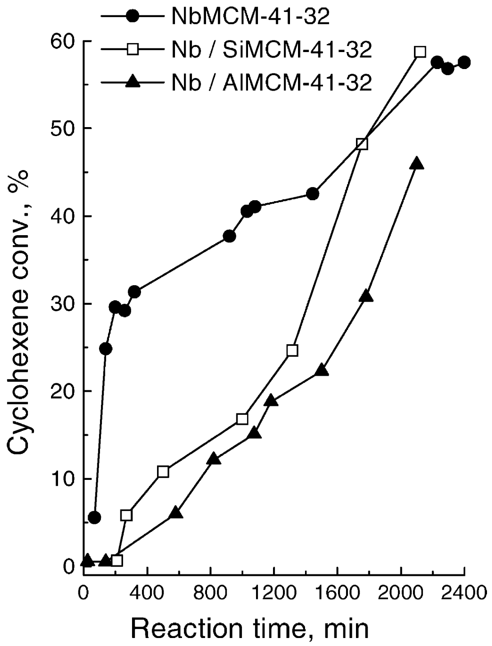

Fig. 7. Cyclohexene conversion dependence on localisation of niobium (framework, extra framework) and the nature of matrix (siliceous, aluminosilicate).

The question has arisen, if the reaction proceeds partially in the homogeneous phase using Nb-containing solids as heterogeneous catalysts. To answer this question some special experiments were carried out. The reactions carried out in homogeneous conditions (by dissolving the same amount of niobium oxalate in acetonitrile as that used for the synthesis of NbMCM-41 catalysts) proceeds with a very low activity and high selectivity to glycol. After few hours of stirring the catalyst—NbMCM-41(NUPS)—with hydrogen peroxide followed by the filtration of the catalysts, the reaction was carried out in the solution leached from catalysts after admission of cyclohexene. It shows only residual activity. There was no activity, when the sample was first stirred with cyclohexene for 5 h, and after removing the catalyst hydrogen peroxide was added to the solution. No reaction was observed in the case of NbMCM-41(UPS) sample stirred with methanol for 20 h, after which the reaction was conducted on the filtrate.

As NO can really change reaction kinetics we studied an epoxidation reaction under a NO atmosphere. NO was introduced during the addition of reagents and for the first 15 min of the reaction. Using a niobium-containing MCM-41(UPS) catalyst and H_2O_2 as oxidant, the conversion decreases from 30 to 5% in methanol and from 40 to almost 0% in acetonitrile even after 10 h of the reaction. It is worthy to note that the selectivity changes completely in methanol as in the absence of NO (after 10 h of the reaction) the main product was epoxide, whereas in the NO atmosphere it was glycol. It is difficult to judge on the changes in the selectivity in acetonitrile, as the conversion in the presence of NO was very low, however, it seems that the product distribution remained unchanged. For NbMCM-41(NUPS) the same behaviour was observed as seen from Fig. 8. This shows that the kinetics of the cyclohexene oxidation in methanol was totally changed, while the kinetics of the epoxidation in acetonitrile was only slightly influenced by some NO coordinated to the active sites of the catalysts. However, the activity drastically decreases suggesting the radical oxidation mechanism [13]. Furthermore, NO also reacts with the reaction intermediate (cyclohexyl radical), thus totally changing the product distribution in the case of methanol.

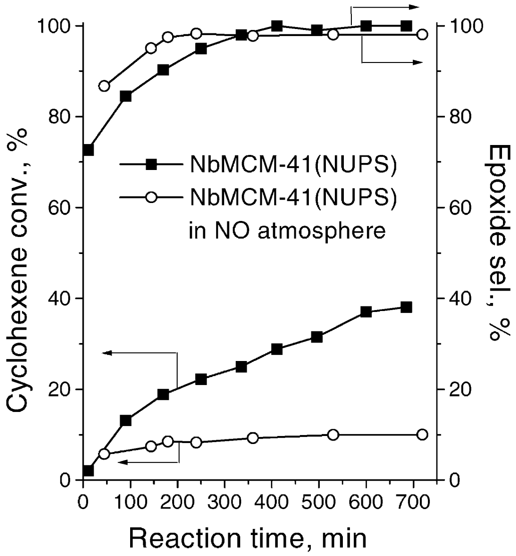

Fig. 8. Influence of NO atmosphere on epoxidation of cyclohexene in acetonitrile.

Lewis acidity in NbMCM-41 [12] seems to participate in the catalytic oxidation of cyclohexene with H_2O_2. The addition of a small amount of water (0.55 mmol) to the reaction medium does not change the initial rate of the reaction and the selectivity. However, the further addition of water (2.2 mmol) decreases significantly the activity suggesting that the Nb sites are partially blocked by water. The reaction proceeds with low conversion in water used as a solvent. Additionally, the main observed product was cyclohex-2-ene-1-ol suggesting an allylic attack via the reaction pathway no. 3 in Scheme 1.

4. Discussion

Four various procedures described in the literature [2,6–8] for the synthesis of M41S family molecular sieves (MCM-41 and MCM-48) have been applied in this work for the preparation of niobosiliceous mesoporous molecular sieves. However, two of the promised procedures, namely hydrothermal synthesis in autoclave at 403 K recommended by Sayari [6] for the production of siliceous MCM-48, and the synthesis of TUD-1 proposed by Maschmeyer and co-workers [9] did not lead to mesoporous materials if niobium salt was used in the syntheses. In both cases macroporous niobosilicates (NbSM-1 and NbSM-2, respectively) have been obtained as evidenced from N_2 adsorption/desorption isotherms. H_2-TPR results suggested the incorporation of Nb into the framework of macroporous NbSM-2. These results indicate that the form of the final material is strongly dependent on the nature of heteroatom used in the syntheses carried out according to [6,9].

4.1. Effect of mesopore size on the oxidation activity

A slight modification (described in Section 2) of the well known procedure for the preparation of NbMCM-41 [5] gives rise to the formation of double mesoporous system as shown in Fig. 4 (NbMCM-41(NUPS)). Consequently, the activity in cyclohexene epoxidation is higher than that noted when NbMCM-41(UPS) is applied. Taking into account the consideration of Haller and co-workers [14] about the influence of T–O–T angle in the walls of mesoporous VMCM-41 molecular sieve on the activity in cyclohexene oxidation, one can suggest that the second pore system (diameter ∼4 nm) in NbMCM-41(NUPS) is responsible for the higher oxidation activity. Si–O–Nb bond angles depend on the pore size. The higher pore size the higher Si–O–Nb bond angles occurs. Mesoporous MCM-41 sieves give an opportunity of changing T–O–T angles without changing of their structures, contrary to zeolites in which T–O–T values strongly limit a kind of structure. The electron density of niobium sites, which may be “tuned” by the pore size through a variation of Si–O–Nb bond angles, affects the effective redox potential of Nb sites and consequently the adsorption bond strength. It is well known in catalysis that the fastest reaction rate is achieved when the bonds between the adsorbed intermediate complex and the catalyst are neither too strong nor too weak. It is very probable that the additional pore system, with a higher diameter, registered in NbMCM-41(NUPS) gives a favourable bond strength between active Nb sites and reactants. Haller and co-workers [14] observed a volcano curve exhibiting the dependence of the oxidation activity on the pore size of VMCM-41 materials. Maybe the same feature will be characteristic of NbMCM-41. The explanation of that requires further studies.

4.2. Diffusion effect

Diffusion limitations and steric constraints due to reactants or transition-state intermediates are the other factors influencing the oxidation activity in the liquid phase. As shown in this paper, the presence of extra framework niobium species in the impregnated materials or in NbSM-1, or NbMCM-41(RT) strongly inhibits the activity in cyclohexene oxidation, especially in the initial stage of the reaction. That is no doubt that the diffusion effect plays an important role on the activity of these materials. However, considering the low activity of macroporous NbSM-1 material one cannot explain that behaviour by the diffusion effect because the average pore size in this sample is very high and the presence of extra framework Nb-species cannot strongly limit the diffusion. In such materials extra framework niobium phases most probably block the active centres localised in the walls of materials.

4.3. Role of acidity

The role of the catalysts surface acid–base properties on the heterogeneously catalysed oxidation reaction mechanism has been stressed by Busca et al. [15]. Acid–base properties depend on the covalent/ionic character of the metal-oxygen bonds and are involved in some steps of the oxidation reactions, such as the activation of the C–H hydrocarbon bonds, the desorption/overoxidation of the partial oxidation products, the opening of the epoxide ring. Thus they participate with the niobium redox properties in determining the selective/unselective catalyst behaviour.

It is known that NbMCM-41 after dehydroxylation exhibited the presence of Lewis acid sites ($Nb^{\delta+}$-coordinatively unsaturated species localised in the framework) [16]. They act as traps for electron–donor molecules. So, they participate in the oxygen transfer, which occurs in the Mars van Krevelen mechanism of the oxidation. The observed poisoning effect of nitric oxide on the catalytic activity is assumed to be due an occupation of the oxygen vacancy by a molecule of NO. This effect confirms the radical mechanism of cyclohexene epoxidation.

The generation of too strong acidic centres on the surface of Nb-materials is unfavourable in the selective oxidation of cyclohexene to epoxide. It is due to the opening of epoxide ring and following the reaction towards a glycol product. Taking this statement into account one can explain the observed difference between the selectivity in cyclohexene epoxidation carried out by us [10] and Xin et al. [4]. The latter prepared NbMCM-41 from niobium(V) chloride whereas we used niobium(V) oxalate. As recently found by one of us [17] the niobium source determines the texture and structure of the material. If chloride is used, a residual acidity in the sample can be observed. This can cause the fast transformation of epoxide to glycol and in a consequence—high glycol selectivity.

4.4. *Stability of niobium*

The stability of Nb in the framework of mesoporous molecular sieves was described earlier [18]. In this work one can compare the stability of NbMCM-41 with that of mesoporous molecular sieves containing vanadium and titanium. Vanadium and titanium are easily leached from the sample to the solution (the medium of a liquid phase oxidation of cyclohexene) whereas niobium is more stable.

5. Conclusions

The method applied for the preparation of Nb-containing M41S family mesoporous molecular sieves strongly affects the characteristics of the final material. It varies from meso-, via meso–macro- to macropores, depending on the procedure. The obtained structure determines the catalytic properties in the epoxidation of cyclohexene.

Acknowledgements

This work was supported by KBN (Polish State Committee for Scientific Research)—grant no. T09A 102 19. Companhia Brasilia de Metalurgia e Mineraçáo is acknowledged for providing a niobium(V) oxalate.

References

[1] C.T. Kresge, M.E. Leonowicz, W.J. Roth, J.C. Vartuli, J.S. Beck, Nature 359 (1992) 710.
[2] J.C. Vartuli, K.D. Schmidt, C.T. Kresge, W.J. Roth, M.E. Leonowicz, S.B. McCullen, S.D. Hellring, J.S. Beck, J.L. Schlenker, D.H. Olson, E.W. Sheppard, Chem. Mater. 6 (1994) 2317.
[3] M. Ziolek, I. Nowak, I. Sobczak, A. Lewandowska, P. Decyk, J. Kujawa, Stud. Surf. Sci. Catal. 129 (2000) 813.
[4] J. Xin, J. Suo, X. Zhang, Z. Zhang, New J. Chem. 24 (2000) 813.
[5] M. Ziolek, I. Nowak, Zeolites 18 (1997) 356.
[6] A. Sayari, J. Am. Chem. Soc. 122 (2000) 6504.
[7] K. Schumacher, M. Grün, K.K. Unger, Micropor. Mesopor. Mater. 27 (1999) 201.
[8] R. Schmidt, M. Stöcker, D. Akporiaye, E.H. Tørstad, A. Olsen, Micropor. Mater. 5 (1995) 1.
[9] Z. Shan, E. Gianotti, J.C. Jansen, J.A. Peters, L. Marchese, T. Maschmeyer, Chem. Eur. J. 7 (2001) 1437–1443.
[10] M. Ziolek, A. Lewandowska, B. Kilos, I. Nowak, in: Proceedings of the Fourth World Oxidation Congress, Potsdam, Book of Extended Abstracts, vol. I, September 16–21, 2001, p. 79.
[11] L.C. Passoni, M.R.H. Siddiqui, A. Steiner, I.V. Kozhevnikov, J. Mol. Catal. A 153 (2000) 103.
[12] M. Ziolek, I. Sobczak, A. Lewandowska, I. Nowak, P. Decyk, M. Renn, B. Jankowska, Catal. Today 70 (2001) 169.
[13] U. Schuchardt, M.J.D.M. Jannini, M.C. Guerreiro, in: Proceedings of the Fourth World Oxidation Congress, Potsdam, Book of Extended Abstracts, vol. II, September 16–21, 2001, p. 383.
[14] D. Wei, W.-T. Chueh, G.L. Haller, Catal. Today 51 (1991) 501.

[15] G. Busca, E. Finocchio, G. Ramis, G. Ricchiardi, Catal. Today 32 (1996) 133.
[16] M. Ziolek, I. Nowak, J.C. Lavalley, Catal. Lett. 45 (1997) 259.
[17] I. Nowak, Stud. Surf. Sci. Catal. 142 (2002) 1363.
[18] M. Ziolek, A. Lewandowska, M. Renn, I. Nowak, Stud. Surf. Sci. Catal. 135 (2001) 366.